

Article

High-Pressure Spectroscopy Study of $\text{Zn}(\text{IO}_3)_2$ Using Far-Infrared Synchrotron Radiation

Akun Liang ¹, Robin Turnbull ¹, Enrico Bandiello ¹, Ibraheem Yousef ², Catalin Popescu ², Zoulikha Hebboul ³ and Daniel Errandonea ^{1,*}

¹ Departamento de Física Aplicada-ICMUV, Universitat de València, Dr. Moliner 50, 46100 Burjassot, Spain; akun2.liang@uv.es (A.L.); robin.turnbull@uv.es (R.T.); enrico.bandiello@uv.es (E.B.)

² CELLS-ALBA Synchrotron Light Facility, 08290 Barcelona, Spain; iyousef@cells.es (I.Y.); cpopescu@cells.es (C.P.)

³ Laboratoire Physico-Chimie des Matériaux (LPCM), Université Amar Telidji de Laghouat, BP 37G, Laghouat 03000, Algeria; z.hebboul@lagh-univ.dz

* Correspondence: daniel.errandonea@uv.es

Abstract: We report the first high-pressure spectroscopy study on $\text{Zn}(\text{IO}_3)_2$ using synchrotron far-infrared radiation. Spectroscopy was conducted up to pressures of 17 GPa at room temperature. Twenty-five phonons were identified below 600 cm^{-1} for the initial monoclinic low-pressure polymorph of $\text{Zn}(\text{IO}_3)_2$. The pressure response of the modes with wavenumbers above 150 cm^{-1} has been characterized, with modes exhibiting non-linear responses and frequency discontinuities that have been proposed to be related to the existence of phase transitions. Analysis of the high-pressure spectra acquired on compression indicates that $\text{Zn}(\text{IO}_3)_2$ undergoes subtle phase transitions around 3 and 8 GPa, followed by a more drastic transition around 13 GPa.

Keywords: iodate; infrared spectroscopy; high pressure; phase transitions



Citation: Liang, A.; Turnbull, R.; Bandiello, E.; Yousef, I.; Popescu, C.; Hebboul, Z.; Errandonea, D. High-Pressure Spectroscopy Study of $\text{Zn}(\text{IO}_3)_2$ Using Far-Infrared Synchrotron Radiation. *Crystals* **2021**, *11*, 34. <https://doi.org/10.3390/cryst11010034>

Received: 17 December 2020

Accepted: 28 December 2020

Published: 30 December 2020

Publisher's Note: MDPI stays neutral with regard to jurisdictional claims in published maps and institutional affiliations.



Copyright: © 2021 by the authors. Licensee MDPI, Basel, Switzerland. This article is an open access article distributed under the terms and conditions of the Creative Commons Attribution (CC BY) license (<https://creativecommons.org/licenses/by/4.0/>).

1. Introduction

Metal iodates $[\text{M}(\text{IO}_3)_x]$ receive great attention because of their non-linear optical properties. In particular, they are promising materials for second-harmonic generation (SHG) [1–4]. They have been also proposed for applications as dielectric materials, in non-linear optics, and for desalination and water treatment [1–4]. Amongst the iodates, the quasi-two-dimensional zinc iodate, $\text{Zn}(\text{IO}_3)_2$, has recently been studied by several research groups [5–8]. The crystal structure, thermal stability, and other physical properties of this compound have been characterized at ambient pressure [9–11]. However, nothing is known of its structural and vibrational behavior under high-pressure (HP) conditions. At ambient conditions, $\text{Zn}(\text{IO}_3)_2$ crystallizes into a monoclinic structure, which is represented in Figure 1. The monoclinic structure consists of ZnO_6 octahedral units connected by IO_3 triangular pyramidal units. In these units, the pentavalent iodine atom forms three covalent bonds with oxygen atoms, leaving two 5s electrons free to act as lone electron pairs (LEP). The presence of the LEP has been shown to induce an interesting HP behavior in iodates related to $\text{Zn}(\text{IO}_3)_2$ like $\text{Fe}(\text{IO}_3)_3$ [12,13], with two isostructural phase transitions taking place at pressures below 10 GPa in this compound. These transitions have been detected from changes in the pressure dependences of phonon frequencies, which show a nonlinear behavior, as well as kinks and slope changes in the frequency-versus-pressure plot at the identified transition pressures [12,13]. Such unusual behavior of phonons has been proposed to be connected with gradual modifications of the iodine coordination, which is favored by the LEP of iodine and has been connected with the isostructural phase transitions discovered in $\text{Fe}(\text{IO}_3)_3$ [12,13]. Since the LEP of iodine is a typical feature of many $\text{M}(\text{IO}_3)_x$ iodates, it would be interesting to explore if low-pressure phase transitions are a typical feature of this family of compounds. Given the structural similarities between

$\text{Fe}(\text{IO}_3)_3$ and $\text{Zn}(\text{IO}_3)_2$ (both structures consist of MO_6 octahedral units connected by iodine atoms coordinated by three oxygen atoms with non-bonding LEP orbitals), the possibility of isostructural phase transitions at low pressures in the unexplored $\text{Zn}(\text{IO}_3)_2$ motivated the present work, in which we studied the pressure dependence of phonons by means of HP infrared (IR) spectroscopy. This is a technique useful for understanding the changes induced by compression in the physical–chemical properties of iodates. Additionally, the discovery of the existence of phase transition in $\text{Zn}(\text{IO}_3)_2$ could be very useful for the development of solid-state cooling technologies, which take advantage of the pressure-induced barocaloric effect [14].

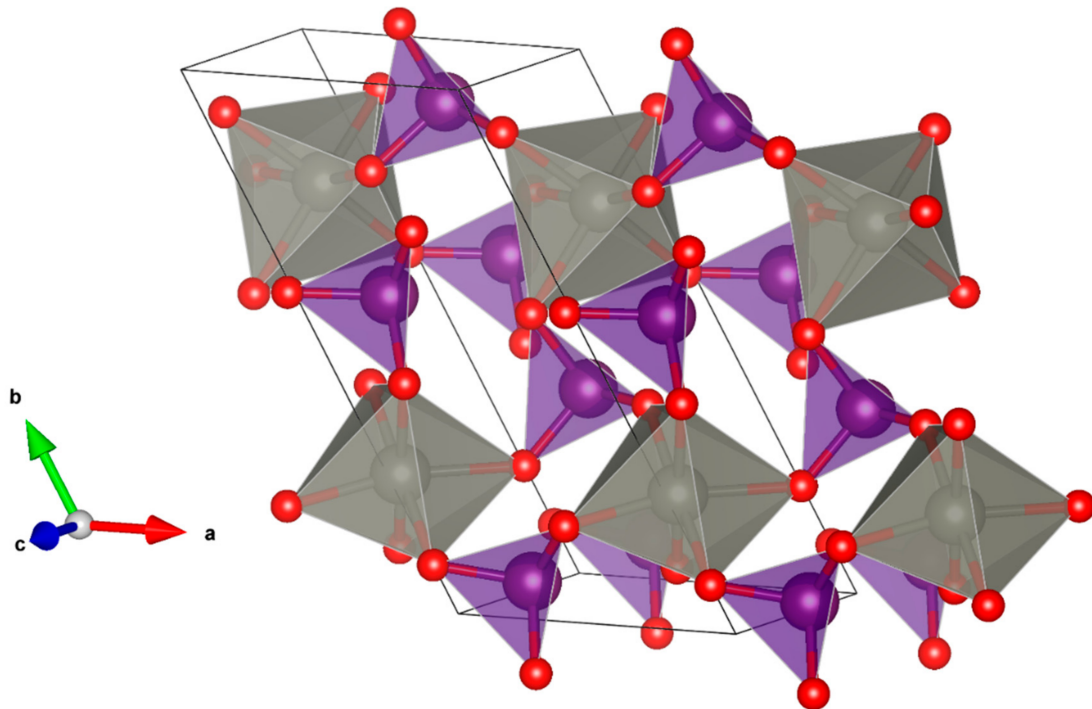


Figure 1. Crystal structure of $\text{Zn}(\text{IO}_3)_2$. ZnO_6 octahedral units are shown in grey and IO_3 trigonal pyramidal units are shown in purple. Small red circles are oxygen atoms. The monoclinic unit cell is shown with black solid lines.

Infrared spectroscopy has been shown to be an effective diagnostic for the detection of pressure-induced phase transitions in solids [15]. In the present work, IR spectroscopy provides information on the vibrational properties of $\text{Zn}(\text{IO}_3)_2$, which, until the present work, have remained relatively underexplored. In fact, less than one-third of the 51 phonons predicted by group theory analysis have been reported experimentally for $\text{Zn}(\text{IO}_3)_2$ [5–9,16]. Therefore, the present far-infrared spectroscopy study of $\text{Zn}(\text{IO}_3)_2$ under high-pressure conditions makes a timely and valuable contribution. $\text{Zn}(\text{IO}_3)_2$ has not previously been studied under high-pressure conditions. The information obtained from this study is relevant not only to improve the knowledge on the aforementioned issues but also to provide an accurate determination of the phonon frequencies, which are needed to properly model other physical properties such as heat capacity and thermal expansion. The use of high-brilliance infrared synchrotron radiation facilitated the measurement of tiny samples loaded in diamond-anvil cells (DACs) with a very good signal-to-noise ratio. Using this methodology, we have been able to identify 25 phonons between 98 and 600 cm^{-1} . We then follow the pressure-induced evolution of these phonons up to 17 GPa. The analysis of the results leads us to propose the existence of three phase transitions, as will be discussed in the manuscript.

2. Materials and Methods

Experiments were performed on $\text{Zn}(\text{IO}_3)_2$ powders synthesized from aqueous solution according to the synthesis method and sample characterization found in Ref. [6]. The crystal structure was confirmed by powder XRD measurements (X'Pert Pro diffractometer, Panalytical, Almelo, The Netherlands) using $\text{Cu K}\alpha_1$ radiation, which corroborated the crystal structure reported by Liang et al. [10] (space group $P2_1$) with unit-cell parameters: $a = 5.465(4)$, $b = 10.952(8)$, $c = 5.129(4)$ Å, and $\gamma = 120.37(8)^\circ$. HP Fourier transform infrared (FTIR) measurements (Vertex 70 spectrometer, Bruker Optik GmbH, Ettlingen, Germany) were conducted at MIRAS beamline of the ALBA synchrotron. $\text{Zn}(\text{IO}_3)_2$ samples were loaded in a DACs designed for IR spectroscopy, using IIAC-diamonds with culets of 300 μm . Stainless-steel gaskets were pre-indented to a thickness of 40 μm and drilled with a hole in the center of 150 μm in diameter. Cesium iodide (CsI) was used as the pressure-transmitting medium (PTM) [17]. The CsI PTM is not quasi-hydrostatic beyond 3 GPa; however, radial pressure gradients were smaller than 1 GPa in the pressure range of this study [18]. CsI was chosen because it has the widest IR transmission window amongst the possible PTMs [18]. Pressure was determined using the ruby scale [19]. Synchrotron-based FTIR-micro-spectroscopy experiments were performed in the transmission mode of operation. We used a masking aperture size of $50 \times 50 \mu\text{m}^2$ and a beam current inside the synchrotron ring of 250 mA. The measurements were performed by employing a 3000 Hyperion microscope coupled to a Vertex 70 spectrometer (Bruker Optik GmbH, Ettlingen, Germany). The microscope was equipped with a helium-cooled bolometer detector optimized for operation in the range covering the far-infrared spectral region. A Mylar beam splitter was used in the spectrometer. Spectra were measured using a $15\times$ Schwarzschild magnification objective ($\text{NA} = 0.52$) coupled to a $15\times$ Schwarzschild magnification condenser. Measurements at selected pressures were collected using the OPUS 8.2 software (Bruker Optik GmbH, Ettlingen, Germany) in the $90\text{--}600 \text{ cm}^{-1}$ range with a spectral resolution of 4 cm^{-1} and 256 co-added scans per spectrum. The analysis of FTIR results was carried using the Multiple Peak Fit Tool of the OriginPro software (OriginLab Corporation, Northampton, MA, United States) and employing Gaussian functions to model the peaks.

3. Results and Discussion

The results at the lowest measured pressure (0.9 GPa) are shown in Figure 2 together with the multiple-peak fit used to identify phonons. We have identified 25 modes, as can be seen in the figure, thereby greatly extending the number of modes previously observed in zinc iodate. The frequencies of all 25 of these modes are summarized in Table 1 and compared with those reported in the literature. $\text{Zn}(\text{IO}_3)_2$ exhibits 51 modes (26A + 25B) according to group theory. All of these 51 modes are both Raman-active and IR-active. They can be described as internal vibrations of the of the IO_3 units and external vibrations (commonly known as lattice modes) involving the relative movements of IO_3 (behaving as rigid units) and Zn, which are observed in the low-frequency region [7,20]. Symmetric (ν_1) and asymmetric (ν_3) stretching vibrations of the pyramidal IO_3 units are in the $780\text{--}630 \text{ cm}^{-1}$ and $820\text{--}730 \text{ cm}^{-1}$ wavenumber regions, respectively [7,21,22]. The symmetric (ν_2) and asymmetric bending vibrations (ν_4) are in the $400\text{--}320 \text{ cm}^{-1}$ wavenumber region and around $450\text{--}400 \text{ cm}^{-1}$, respectively [7,21,22]. In our experiments, we detected four ν_4 modes. The frequencies of the modes we found at 425, 440, and 452 cm^{-1} are less than 9 cm^{-1} larger than those measured in previous ambient-pressure Raman and IR experiments [6,7,16]. This is consistent with the fact that our experiment was performed at a pressure of 0.9 GPa. The expected phonon hardening [23], or increase in the phonon frequency, is due to the shortening bond distance caused by increasing pressure in our experiment. The mode reported at 405 cm^{-1} in Ref. [5] was not detected in previous works from the literature, but in our case could be probably assigned to a shoulder of the peak with wavenumber 388 cm^{-1} , which can be identified at 402 cm^{-1} . Additionally, the mode previously reported at 524 cm^{-1} in Ref. [8] is not consistent either with the present

or previous experiments [5–7,16]. Indeed, there are no phonons in $\text{Zn}(\text{IO}_3)_2$, or in any divalent metal iodate [7], in the $600\text{--}500\text{ cm}^{-1}$ range. The origin of such a phonon could be related with twinning of the crystal structure when large single crystals are grown [9], being a possible overtone, since 524 cm^{-1} is approximately double of the frequency of the lattice modes.

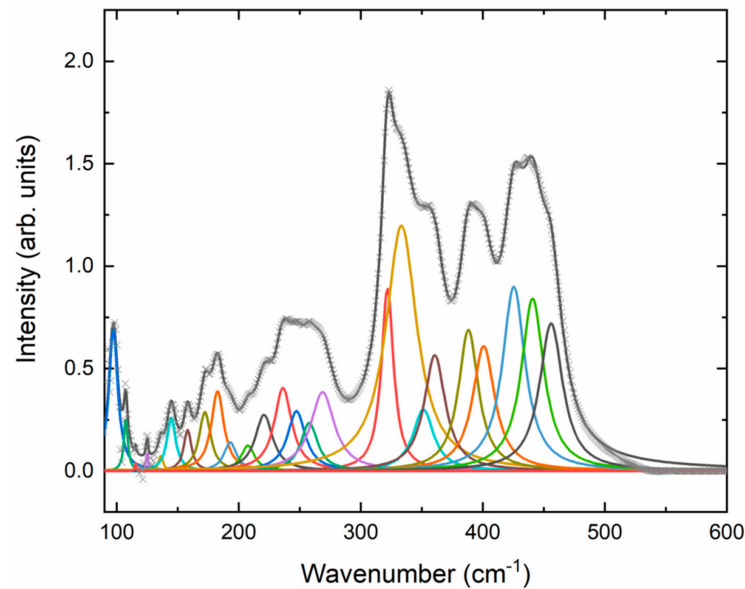


Figure 2. Far-IR spectrum of $\text{Zn}(\text{IO}_3)_2$ measured at 0.9 GPa and room temperature. The Gaussians used for the multiple peak fit are also shown in different colors. Each of them corresponds to the phonons summarized in Table 1.

Table 1. A comparison of the phonon frequencies determined by IR- and Raman-spectroscopy from this work (at 0.9 GPa) and from previous studies (ambient pressure). For the present study, frequencies are given with errors. The horizontal dashed line indicates the cut-off of the IR set-up, below which it was not possible to detect signal due to experimental constraints.

Assignment	$\omega\text{ (cm}^{-1}\text{)}$ This Work IR	$\omega\text{ (cm}^{-1}\text{)}$ [5] IR	$\omega\text{ (cm}^{-1}\text{)}$ [6] IR	$\omega\text{ (cm}^{-1}\text{)}$ [7] IR	$\omega\text{ (cm}^{-1}\text{)}$ [7] Raman	$\omega\text{ (cm}^{-1}\text{)}$ [8] IR>	$\omega\text{ (cm}^{-1}\text{)}$ [16] Raman
							61
							67
				73			80
	98(2)				80		80
	107(2)			101			100
	116(2)				113		111
	125(2)						
	135(2)				132		139
Lattice modes	145(2)			141			148
	158(2)				152		155
	172(2)				173		173
	183(2)			180			
	193(2)				189		187
	208(2)						
	220(2)						
	236(2)						
	247(2)						
	258(2)			255			
	269(2)				267		265

Table 1. Cont.

Assignment	ω (cm ⁻¹) This Work IR	ω (cm ⁻¹) [5] IR	ω (cm ⁻¹) [6] IR	ω (cm ⁻¹) [7] IR	ω (cm ⁻¹) [7] Raman	ω (cm ⁻¹) [8] IR>	ω (cm ⁻¹) [16] Raman
ν_2	322(2)			327	327		327
	336(2)						
	348(2)						
	353(2)			354	354		351
	388(2)	366				391	
ν_4	402(2)	405					
	425(2)		418	418	424		422
	440(2)						432
	452(2)		444				
						524	

Regarding the other bending vibrations, five ν_2 modes were detected in our experiments. The frequencies of three of them agree well with previous studies [6,7,16], with ours observed at 3–5 cm⁻¹ higher frequencies due to the higher pressure (0.9 GPa) in the sample. The brilliance and resolution of the experimental set-up enabled the identification of two modes that were previously undetected. Additionally, the mode reported at 366 cm⁻¹ in Ref. [5] was not observed in our measurements, and it was not reported in the rest of the works in the literature [6–8,16]. We note that the frequency of this mode is approximately double the frequency of the 183 cm⁻¹ mode detected in the present work and elsewhere in the literature [6–8,16] and that it is therefore likely to be an overtone.

Regarding the lattice modes, sixteen in total were observed. Ten of these modes have been detected in previous studies [7,16], thereby providing good agreement with the results of the present work (especially considering the frequency increase due to the 0.9 GPa experimental sample pressure). In the literature, four modes have been detected by Raman and IR spectroscopy [7,8,16], which could be detected in our experiment because it is below the cut-off frequency of our setup. Lattice modes are mainly related to translation and libration movements of IO₃, and the coupling of these movements with movements of Zn atoms. In particular, the 145 cm⁻¹ phonon has been assigned to a O–Zn–O deformation of the ZnO₆ octahedron [8]. This is consistent with the fact that a mode involving the same deformation of ZnO₆ has the same frequency in ZnWO₄ [24] and ZnMoO₄ [25]. Additionally, the modes below 120 cm⁻¹ are likely to be due to pure translational or librational movements of IO₃, because of the large mass of the iodine atom. This hypothesis is consistent with the observation that these modes have nearly the same frequency in Mn(IO₃)₂, Ni(IO₃)₂, Co(IO₃)₂, and Zn(IO₃)₂ [8] as well as in Fe(IO₃)₃ [10].

We will now comment on the data acquired at higher pressures. For the sake of accuracy, we will concentrate on wavenumbers higher than 150 cm⁻¹ because the signals at lower energy became noisy with increasing pressure. Figure 3 displays IR spectra measured at different pressures (indicated in the figure). It is clear in Figure 3 that there are qualitative changes in the spectra at 3.6 GPa, in particular for wavelengths smaller than 300 cm⁻¹. In particular, three modes (marked by asterisks) increase in intensity. The transition pressure is close to the loss hydrostaticity of the pressure medium (3 GPa) [18]. The influence of non-hydrostaticity in phase transitions induced by pressure in Zn(IO₃)₂ is beyond the scope of this study. Additional changes occur in the IR spectra at 8.8 GPa. In particular, several modes broaden, and three low-frequency modes (also marked with asterisks) become enhanced. Finally, there is a considerable broadening of phonon bands at 13 GPa and higher pressures. Similar changes have been assigned to phase transitions in the case of Fe(IO₃)₃ [12,13]. Thus, phase transitions could be the cause of the changes observed in the IR spectra. Further evidence supporting the existence of phase transitions

in $\text{Zn}(\text{IO}_3)_2$ is obtained via the analysis of the pressure dependence of the mode frequencies described immediately below.

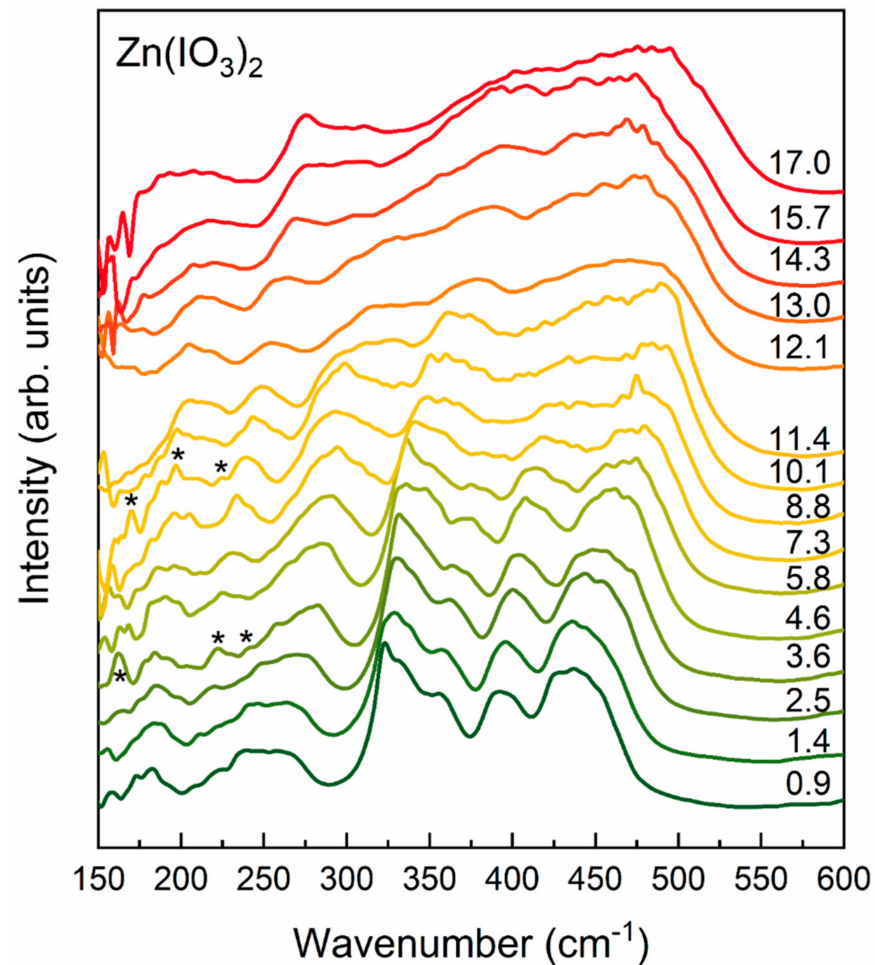


Figure 3. IR spectra acquired at increasing pressures (indicated in GPa in the figure). The asterisks indicate changes in the phonons described in the text.

From the analysis of the HP experiments, we determined the pressure dependence of eight internal bending modes and ten lattice modes. The results are shown in Figures 4 and 5. In Figure 4, it can be clearly seen that there are changes, at 3.6 and 8.8 GPa, in the pressure dependence of several modes; in particular, the bending modes with frequencies of 360 and 440 cm^{-1} among others. There are also clear changes in the modes with frequency 353 and 425 cm^{-1} at 8.8 GPa. On top of this, at 13 GPa, there are noticeable changes in the eight bending modes shown in Figure 4. In particular, there are discontinuities in at least two of the frequencies, indicating the occurrence of more important structural changes in the third phase transition than in the other two transitions.

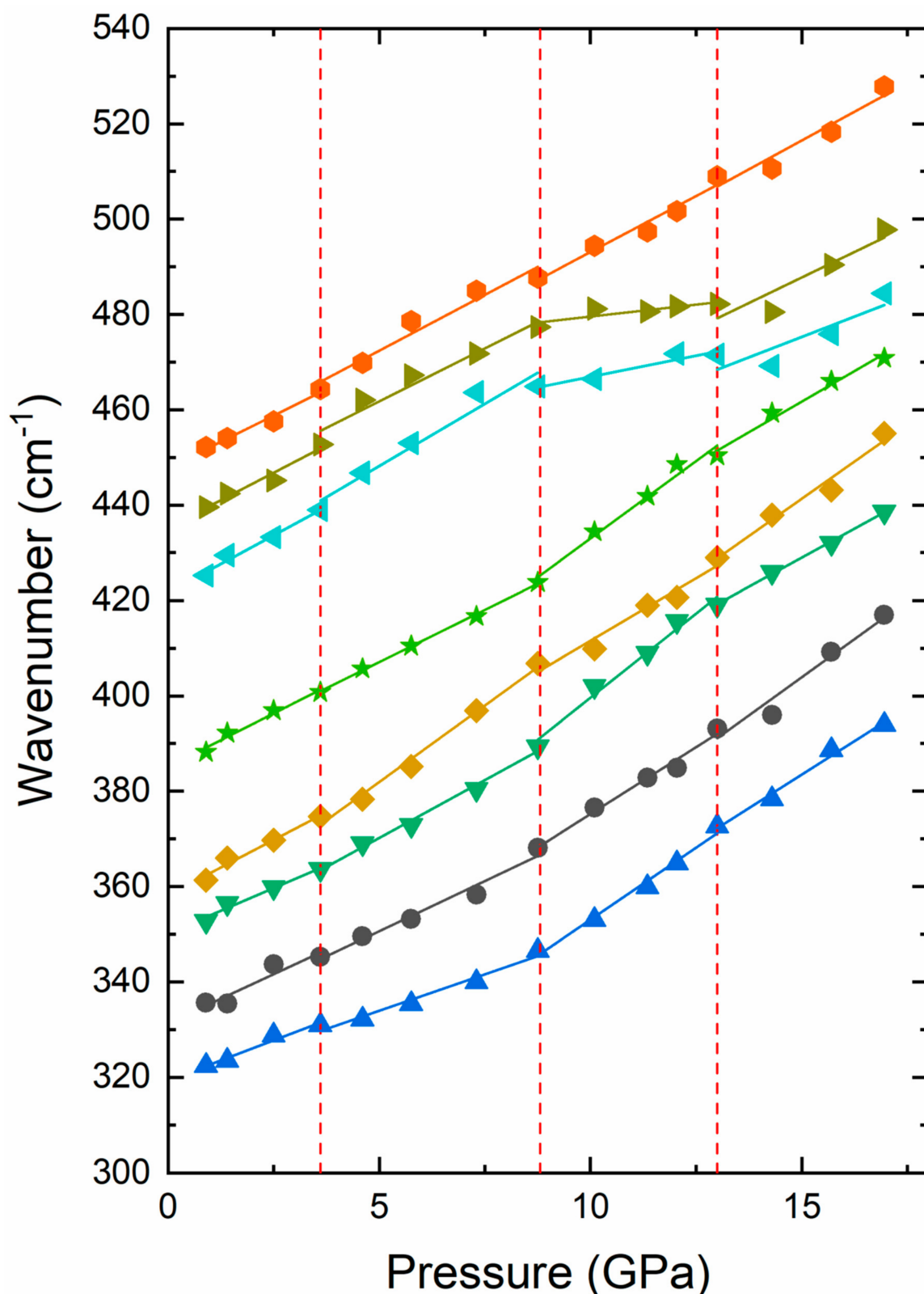


Figure 4. Pressure dependence of IR modes obtained from experiments. Only IO₃ internal bending modes are shown. Vertical lines indicate suggested transition pressures.

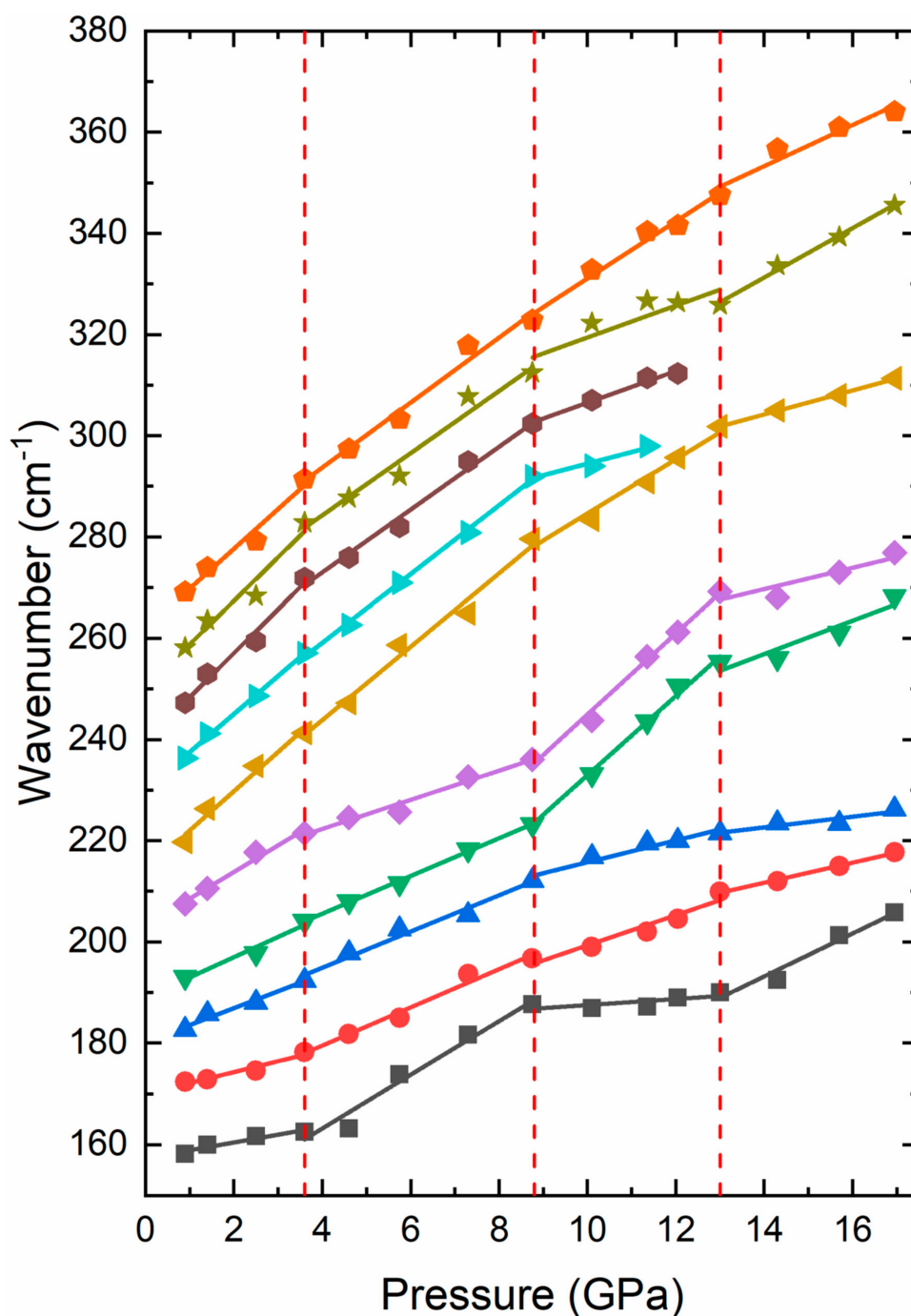


Figure 5. Pressure dependence of IR modes obtained from experiments. Only lattice modes are shown. Vertical lines indicate suggested transition pressures.

We will comment now on the pressure dependence of the ten lattice modes that were observed under sample compression. For these modes, the changes in the frequency pressure dependence, at phase transitions, are more evident than in the bending modes, as can be seen in Figure 5. In particular, slope changes can be seen at the transition pressures (3.6, 8.8, and 13 GPa), which are represented by vertical lines in the figure. Such changes are very noticeable in the lowest-frequency mode shown in Figure 5. They are also quite evident for the mode at 208 cm^{-1} at 0.9 GPa. As happened in the bending modes, the changes at 13 GPa are more noticeable than changes at the other transitions. In particular, there are discontinuities in the frequencies of at least two modes. The changes in the frequency pressure dependences at the phase transitions detected at 3.6 and 8.8 GPa, and

the strongly non-linear pressure dependences, are qualitatively similar to those observed for phonons in $\text{Fe}(\text{IO}_3)_3$ at 2 and 6 GPa [12,13]. In $\text{Fe}(\text{IO}_3)_3$, these changes have been related to isostructural phase transitions occurring in Ref. [12,13], which are themselves related to gradual pressure-induced changes in the coordination sphere of iodine, which are affected by the presence of lone electron pairs. The similarities between $\text{Zn}(\text{IO}_3)_2$ and $\text{Fe}(\text{IO}_3)_3$ therefore provide further support to the observation of phase transitions in the $\text{Zn}(\text{IO}_3)_2$ investigated here. Future studies using other characterization techniques, including X-ray diffraction and Raman spectroscopy should be performed to confirm the present interpretation of results and to determine if the transitions at 3.6 and 8.8 GPa are isostructural or not. We hope our work will trigger such studies as well as computer simulation studies.

Before concluding, we would like to add a comment on the transition at 13 GPa. The changes observed around 13 GPa are more apparent than those observed around 3.6 and 8.8 GPa. This suggests that the changes around 13 GPa can be linked to the occurrence of a first-order structural transition. The fact that the changes are accompanied by a marked broadening of phonon bands suggests a disorder of the crystal structure [26], which could be related to the presence of non-hydrostatic stresses at 13 GPa and higher pressures [27].

To conclude, we note that all observed modes harden under compression. In the pressure range up to 3.6 GPa (before the first phase transition), the pressure coefficients are all within the range of $1\text{--}9\text{ cm}^{-1}/\text{GPa}$. This can be seen in Table 2, where we represent phonons frequencies (ω) and pressure coefficients ($d\omega/dP$) for different modes in the different phases. We have named the phases as follows: phase I (low-pressure phase), II, III, and IV (successive HP phases). Table 2 shows clearly the change in the pressure dependences at 3.6 GPa and 8.8 GPa as well as the changes in frequencies and pressure dependencies at 13 GPa, supporting the existence of the proposed transitions. The pressure coefficients in the low-pressure phase are comparable to pressure coefficients in $\text{Fe}(\text{IO}_3)_3$ [13], LiIO_3 [28], and KIO_3 [29] in the same frequency region, indicating that $\text{Zn}(\text{IO}_3)_2$ is extremely compressible, similar to these other iodates. Additionally, the pressure coefficients for the different HP phases are of the same order of magnitude as in the low-pressure phase, suggesting that the changes in the coordination polyhedra are not drastic and that the transition is probably related to gradual changes in cation coordination number [30].

Table 2. Phonon frequencies (ω) of the modes observed under compression for phases I (at 0.9 GPa), II (at 3.6 GPa), III (at 8.8 GPa), and IV (at 13 GPa). The pressure coefficients ($d\omega/dP$) obtained from linear fits are also given.

ω (cm^{-1}) Phase I 0.9 GP	$d\omega/dP$ ($\text{cm}^{-1}/\text{GPa}$)	ω (cm^{-1}) Phase II 3.6 GPa	$d\omega/dP$ ($\text{cm}^{-1}/\text{GPa}$)	ω (cm^{-1}) Phase III 8.8 GPa	$d\omega/dP$ ($\text{cm}^{-1}/\text{GPa}$)	ω (cm^{-1}) Phase IV 13 GPa	$d\omega/dP$ ($\text{cm}^{-1}/\text{GPa}$)
158(2)	1.5(1)	163(2)	5.3(1)	188(2)	0.6(1)	190(2)	4.2(1)
172(2)	2.1(1)	178(2)	3.8(1)	197(2)	3.0(1)	210(2)	2.0(1)
183(2)	3.3(1)	192(2)	3.6(1)	212(2)	2.2(1)	222(2)	1.1(1)
193(2)	4.0(1)	204(2)	3.7(1)	223(2)	7.8(1)	255(2)	3.3(1)
207(2)	5.3(1)	221(2)	2.9(1)	236(2)	8.0(1)	269(2)	2.1(1)
220(2)	7.8(1)	241(2)	7.2(1)	280(2)	5.3(1)	302(2)	2.4(1)
236(2)	7.5(1)	257(2)	6.8(1)	292(2)	2.3(1)	–	–
247(2)	8.7(1)	272(2)	6.2(1)	302(2)	3.1(1)	–	–
258(2)	8.6(1)	283(2)	6.1(1)	312(2)	3.2(1)	326(2)	4.9(1)
269(2)	7.9(1)	291(2)	6.4(1)	323(2)	5.7(1)	348(2)	4.1(1)
322(2)	4.1(1)	331(2)	4.2(1)	347(2)	5.6(1)	373(2)	6.4(1)
336(2)	3.4(1)	345(2)	3.1(1)	368(2)	6.0(1)	393(2)	5.6(1)
353(2)	3.8(1)	364(2)	4.9(1)	389(2)	7.1(1)	419(2)	4.9(1)
361(2)	4.6(1)	375(2)	6.4(1)	407(2)	5.2(1)	429(2)	6.3(1)
388(2)	4.8(1)	401(2)	5.2(1)	424(2)	1.8(1)	450(2)	3.4(1)
425(2)	4.6(1)	439(2)	4.4(1)	465(2)	0.5(1)	471(2)	4.3(1)
440(2)	4.4(1)	453(2)	4.7(1)	477(2)	0.7(1)	482(2)	4.8(1)
452(2)	4.5(1)	464(2)	4.4(1)	488(2)	6.5(1)	509(2)	5.1(1)

4. Conclusions

Synchrotron far-infrared spectroscopy measurements have allowed us to determine that $\text{Zn}(\text{IO}_3)_2$ undergoes three phase transitions at 3.6, 8.8, and 13 GPa. The phase transitions are identified from changes in the infrared spectra. The first two transitions resemble those previously observed in $\text{Fe}(\text{IO}_3)_3$ at similar pressures and are probably isostructural transitions favored by the presence of lone electron pairs in $\text{Zn}(\text{IO}_3)_2$. The third phase transition appears to be a first-order transition that is connected to the occurrence of more important structural changes. Assignment of phonon modes has been discussed and their pressure dependence reported. We found that the lattice modes are more sensitive than the bending modes of IO_3 to pressure-induced structural changes.

Author Contributions: Conceptualization, D.E.; IR experiments, A.L., R.T., E.B., I.Y., and C.P.; formal analysis, A.L. and D.E.; sample preparation, Z.H.; writing, review, and editing, all the authors. All authors have read and agreed to the published version of the manuscript.

Funding: This work was supported by the Spanish Ministry of Science, Innovation, and Universities under grants PID2019-106383GB-C41 and RED2018-102612-T (MALTA Consolider-Team Network) and by Generalitat Valenciana under grant Prometeo/2018/123 (EFIMAT). R.T. acknowledges funding from the Spanish MINECO via the Juan de la Cierva Formación program (FJC2018-036185-I). A.L. and D.E. would like to thank the Generalitat Valenciana for the Ph.D. fellowship GRISO-LIAP/2019/025.

Institutional Review Board Statement: Not applicable.

Informed Consent Statement: Not applicable.

Data Availability Statement: Data is contained within the article.

Acknowledgments: The authors thank ALBA synchrotron for providing beamtime at MIRAS beamline for performing synchrotron far-infrared experiments.

Conflicts of Interest: The authors declare no conflict of interest.

References

1. Bonacina, L.; Mugnier, Y.; Courvoisier, F.; Le Dantec, R.; Extermann, J.; Lambert, Y.; Boutou, V.; Galez, C.; Wolf, J.P. Polar $\text{Fe}(\text{IO}_3)_3$ nanocrystals as local probes for nonlinear microscopy. *Appl. Phys. B Lasers Opt.* **2007**, *87*, 399–403. [[CrossRef](#)]
2. Hebboul, Z.; Galez, C.; Benbortal, D.; Beauquis, S.; Mugnier, Y.; Benmakhlouf, A.; Bouchenafa, M.; Errandonea, D. Synthesis, characterization, and crystal structure determination of a new lithium zinc iodate polymorph $\text{LiZn}(\text{IO}_3)_3$. *Crystals* **2019**, *9*, 464. [[CrossRef](#)]
3. Jia, Y.J.; Chen, Y.G.; Guo, Y.; Guan, X.F.; Li, C.; Li, B.; Liu, M.M.; Zhang, X.M. $\text{LiM}_{\text{II}}(\text{IO}_3)_3$ ($\text{M}_{\text{II}} = \text{Zn}$ and Cd): Two Promising Nonlinear Optical Crystals Derived from a Tunable Structure Model of $\alpha\text{-LiIO}_3$. *Angew. Chemie Int. Ed.* **2019**, *58*, 17194–17198. [[CrossRef](#)] [[PubMed](#)]
4. Hebboul, Z.; Ghozlane, A.; Turnbull, R.; Benghia, A.; Allaoui, S. Simple new method for the preparation of $\text{La}(\text{IO}_3)_3$ nanoparticles. *Nanomaterials* **2020**, *10*, 2400. [[CrossRef](#)] [[PubMed](#)]
5. Patil, A.B. FTIR study of second group iodate crystals grown by gel method. *Int. J. Grid Nad. Distrib. Comput.* **2020**, *13*, 227–235.
6. Benghia, A.; Hebboul, Z.; Chikhaoui, R.; Khaldoun Lefkaier, I.; Chouireb, A.; Goumri-Said, S. Effect of iodic acid concentration in preparation of zinc iodate: Experimental characterization of $\text{Zn}(\text{IO}_3)_2$, and its physical properties from density functional theory. *Vacuum* **2020**, *181*, 109660. [[CrossRef](#)]
7. Kochuthresia, T.C.; Gautier-Luneau, I.; Vaidyan, V.K.; Bushiri, M.J. Raman and Ftir Spectral Investigations of Twinned $\text{M}(\text{IO}_3)_2$ ($\text{M} = \text{Mn}$, Ni , Co , AND Zn) Crystals. *J. Appl. Spectrosc.* **2016**, *82*, 941–946. [[CrossRef](#)]
8. Shanmuga Sundar, G.J.; Kumar, S.M.R.; Packiya raj, M.; Selvakumar, S. Synthesis, growth, optical, mechanical and dielectric studies on NLO active monometallic zinc iodate [$\text{Zn}(\text{IO}_3)_2$] crystal for frequency conversion. *Mater. Res. Bull.* **2019**, *112*, 22–27. [[CrossRef](#)]
9. Phanon, D.; Bentría, B.; Jeanneau, E.; Benbortal, D.; Mosset, A.; Gautier-Luneau, I. Crystal structure of $\text{M}(\text{IO}_3)_2$ metal iodates, twinned by pseudo-merohedry, with MII: MgII , MnII , CoII , NiII and ZnII . *Z. Krist.* **2006**, *221*, 635–642.
10. Liang, J.K.; Wang, C.G. The structure of $\text{Zn}(\text{IO}_3)_2$ Crystal. *Acta Chim. Sin.* **1982**, *40*, 985–993.
11. Mougél, F.; Kahn-Harari, A.; Aka, G.; Pelenc, D. Structural and thermal stability of Czochralski grown GdCOB oxoborate single crystals. *J. Mater. Chem.* **1998**, *8*, 1619–1623. [[CrossRef](#)]
12. Liang, A.; Rahman, S.; Saqib, H.; Rodriguez-Hernandez, P.; Munoz, A.; Nenert, G.; Yousef, I.; Popescu, C.; Errandonea, D. First-Order Isostructural Phase Transition Induced by High-Pressure in $\text{Fe}(\text{IO}_3)_3$. *J. Phys. Chem. C* **2020**, *124*, 8669–8679. [[CrossRef](#)]

13. Liang, A.; Rahman, S.; Rodriguez-Hernandez, P.; Muñoz, A.; Manjón, F.J.; Nenert, G.; Errandonea, D. High-pressure Raman study of Fe(IO₃)₃: Soft-mode behavior driven by coordination changes of iodine atoms. *J. Phys. Chem. C* **2020**, *124*, 21329–21337. [[CrossRef](#)]
14. Sagotra, A.K.; Errandonea, D.; Cazorla, C. Mechanocaloric effects in superionic thin films from atomistic simulations. *Nat. Commun.* **2017**, *8*, 963. [[CrossRef](#)] [[PubMed](#)]
15. Ross, N.L.; Detrie, T.A.; Liu, Z. High-pressure raman and infrared spectroscopic study of prehnite. *Minerals* **2020**, *10*, 312. [[CrossRef](#)]
16. Peter, S.; Pracht, G.; Lange, N.; Lutz, H.D. Zinkiodate ± Schwingungsspektren (IR, Raman) und Kristallstruktur von Zn(IO₃)₂·2H₂O Zinc Iodates ± Infrared and Raman Spectra, Crystal Structure. *Z. Anorg. Allg. Chem.* **2000**, *626*, 208–215. [[CrossRef](#)]
17. Asaumi, K.; Kondo, Y. Effect of very high pressure on the optical absorption spectra in CsI. *Solid State Commun.* **1981**, *40*, 715–718. [[CrossRef](#)]
18. Celeste, A.; Borondics, F.; Capitani, F. Hydrostaticity of pressure-transmitting media for high pressure infrared spectroscopy. *High Press. Res.* **2019**, *39*, 608–618. [[CrossRef](#)]
19. Mao, H.K.; Xu, J.; Bell, P.M. Calibration of the ruby pressure gauge to 800 kbar under quasi-hydrostatic conditions. *J. Geophys. Res.* **1986**, *91*, 4673–4676. [[CrossRef](#)]
20. Bushiri, M.J.; Kochuthresia, T.C.; Vaidyan, V.K.; Gautier-Luneau, I. Raman scattering structural studies of nonlinear optical M(IO₃)₃ (M = Fe, Ga, and In) and linear optical β-In(IO₃)₃. *J. Nonlinear Opt. Phys. Mater.* **2014**, *23*, 1450039. [[CrossRef](#)]
21. Crettez, J.M.; Gard, R.; Remoissenet, M. Near and far infrared investigations from α and β lithium iodate crystals. *Solid State Commun.* **1972**, *11*, 951–954. [[CrossRef](#)]
22. Pimenta, M.A.; Oliveira, M.A.S.; Bourson, P.; Crettez, J.M. Raman study of Li_{1-x}H_xIO₃ crystals. *J. Phys. Condens. Matter* **1997**, *9*, 7903–7912. [[CrossRef](#)]
23. Errandonea, D.; Muñoz, A.; Rodríguez-Hernández, P.; Gomis, O.; Achary, S.N.; Popescu, C.; Patwe, S.J.; Tyagi, A.K. High-Pressure Crystal Structure, Lattice Vibrations, and Band Structure of BiSbO. *Inorg. Chem.* **2016**, *55*, 4958–4969. [[CrossRef](#)] [[PubMed](#)]
24. Errandonea, D.; Manjón, F.J.; Garro, N.; Rodríguez-Hernández, P.; Radescu, S.; Mujica, A.; Muñoz, A.; Tu, C.Y. Combined Raman scattering and ab initio investigation of pressure-induced structural phase transitions in the scintillator ZnWO₄. *Phys. Rev. B Condens. Matter Mater. Phys.* **2008**, *78*, 054116. [[CrossRef](#)]
25. Cavalcante, L.S.; Moraes, E.; Almeida, M.A.P.; Dalmaschio, C.J.; Batista, N.C.; Varela, J.A.; Longo, E.; Siu Li, M.; Andrés, J.; Beltrán, A. A combined theoretical and experimental study of electronic structure and optical properties of β-ZnMoO₄ microcrystals. *Polyhedron* **2013**, *54*, 13–25. [[CrossRef](#)]
26. Tschauer, O.; Errandonea, D.; Serghiou, G. Possible superlattice formation in high-temperature treated carbonaceous MgB₂ at elevated pressure. *Physica B* **2006**, *371*, 88–94. [[CrossRef](#)]
27. Errandonea, D.; Meng, Y.; Somayazulu, M.; Häusermann, D. Pressure-induced → ω transition in titanium metal: A systematic study of the effects of uniaxial stress. *Physica B* **2005**, *355*, 116–125. [[CrossRef](#)]
28. Mendes Filho, J.; Lemos, V.; Cerdeira, F.; Katiyar, R.S. Raman and x-ray studies of a high-pressure phase transition in β-LiIO₃ and the study of anharmonic effects. *Phys. Rev. B* **1984**, *30*, 7212–7218. [[CrossRef](#)]
29. Shen, Z.X.; Wang, X.B.; Tang, S.H.; Li, H.P.; Zhou, F. High pressure raman study and phase transitions of KIO₃ non-linear optical single crystals. *Rev. High Press. Sci. Technol. No Kagaku To Gijutsu* **1998**, *7*, 751–753. [[CrossRef](#)]
30. Sans, J.A.; Vilaplana, R.; Lora da Silva, E.; Popescu, C.; Cuenca-Gotor, V.P.; Andrada-Chacoón, A.; Muñoz, A.; Sánchez-Benitez, J.; Gomis, O.; Pereira, A.L.J.; et al. Characterization and decomposition of the natural van der Waals SnSb₂Te₄ under compression. *Inorg. Chem.* **2020**, *59*, 9900–9918. [[CrossRef](#)]